

Complexity of Holocene Climate as Reconstructed from a Greenland Ice Core

S. R. O'Brien,*† P. A. Mayewski,† L. D. Meeker, D. A. Meese,
M. S. Twickler, S. I. Whitlow

Glaciochemical time series developed from Summit, Greenland, indicate that the chemical composition of the atmosphere was dynamic during the Holocene epoch. Concentrations of sea salt and terrestrial dusts increased in Summit snow during the periods 0 to 600, 2400 to 3100, 5000 to 6100, 7800 to 8800, and more than 11,300 years ago. The most recent increase, and also the most abrupt, coincides with the Little Ice Age. These changes imply that either the north polar vortex expanded or the meridional air flow intensified during these periods, and that temperatures in the mid to high northern latitudes were potentially the coldest since the Younger Dryas event.

Our ability to predict the environmental consequences of anthropogenic emissions first requires a thorough understanding of natural atmospheric and climatic variability. Records from Summit, Greenland, ice cores reveal that climate variability was markedly more subdued during the Holocene epoch of the Cenozoic era than it was during the last glaciation (1–3). Despite this, the Holocene is known to have significant climatic diversity (4–6). By examining the glaciochemical time series developed from the Greenland Ice Sheet Project 2 (GISP2) ice core, Summit, Greenland (72.6°N, 38.5°W, 3200-m elevation), we reconstructed a precisely dated, continuous chronology of atmospheric and environmental change for the high northern latitudes during the Holocene.

The Holocene is defined in the GISP2 ice core as beginning at the termination of the Younger Dryas (YD) event ~11,600 years before present (years B.P.) (7). We determined chemical concentrations for the 5114 Holocene samples by ion chromatography (8) at an approximate biannual sampling interval. These concentrations were used in a statistical model to estimate changes in the fluxes of marine [sea salt (ss)Na, ssCl, ssMg, ssK, ssCa] and terrestrial [non-sea salt (nss)Na, nssMg, nssK, nssCa] species on the basis of the relative abundance of

each species in sea water (9) (Fig. 1).

Changes in chemical flux values are believed to represent changes in the atmospheric composition over Summit. On the basis of previous investigations of the GISP2 glaciochemical series (3, 10), a greater atmospheric aerosol loading of marine and terrestrial source species existed during the YD event and during glacial portions of the record than during the Holocene (see ssNa profile in Fig. 1). In addition, relative to the glacial portion of the record, GISP2 chemical variations during the Holocene are of lower magnitude. These variations are, however, still sufficient to detect significant changes in environmental conditions.

We used an empirical orthogonal function (EOF) decomposition (11) to quantify the common behavior among Holocene marine and terrestrial source species. In previous GISP2 investigations covering the last 41,000 years of record, it was proposed that EOF1 (the first and dominant EOF) reflects a well-mixed “background” atmosphere representing 92% of the total variance in species behavior over Summit (3). The time series describing the behavior of the well-mixed atmosphere (represented by EOF1) is referred to as the polar circulation index (3) and is believed to provide a measure of the relative size of the polar vortex and the overall intensity of polar atmospheric circulation.

The Holocene EOF1 (Fig. 1) represents 36% of the total variance in the chemical assemblage that includes ssNa, nssNa, nssK, nssCa, nssMg, and NH₄. Less than 10% of the variance in the NH₄ series is explained in the EOF1; NH₄ is therefore addressed separately by Meeker *et al.* (12). Because the Holocene EOF1 represents notably less variance than is represented in our analysis of the last 41,000 years of record (3), we assume that changes in source area, source strength, and atmospheric circulation are more complex in the Holocene.

The EOF1 profile decreases toward the present, primarily because of declining values in the nssCa and nssMg series. This trend in the nssCa and nssMg profiles is believed to represent a gradual decrease in the area of exposed continental shelves as sea level rose during the Holocene (Fig. 1) (13, 14). The thermal contrast between seasons also decreased during the Holocene (milder winters and cooler summers; Fig. 1). This trend may have influenced the glaciochemical trends. For example, changes in landmass heating (resulting from changes in insolation) reportedly altered hydrologic conditions in the eastern Mediterranean region ~6000 and ~9000 years B.P. (15, 16) such that conditions at 9000 years B.P. were even drier than those at 6000 years B.P. (17). Such arid conditions likely increased dust deflation and enhanced atmospheric dust loading over the Northern Hemisphere (as observed at Summit).

Noticeable increases in Holocene EOF1 values occur at 0 to 610, 5000 to 6100, and >11,300 years B.P., and increases of lesser magnitude occur at 2400 to 3100 and 7800 to 8800 years B.P. Concentrations of marine source species in particular increased during these five periods (Fig. 1). Some models have indicated that atmospheric circulation was more zonal when ice sheets were present over North America (18). However, Lamb has suggested that atmospheric circulation patterns during the Little Ice Age (LIA) were more meridional than patterns today (19). Furthermore, the modern-day peak of sea salt in Greenland snow occurs in winter (20), when meridional air flow is intensified (21). Thus, winter-like meteorological conditions (north polar vortex expansion or enhanced meridional circulation) appear consistent with increased concentrations of sea salt species in Summit snow. We suggest, therefore, that cooler climates reoccurred at quasi-2600-year intervals during the Holocene (Fig. 1). The oldest of these events, the >11,300-year increase, is related to circulation patterns associated with the YD event. The most recent increase in sea salt concentration in our record corresponds in timing to the LIA event. Notably, this has the most abrupt onset of any in our Holocene record (Fig. 1). Milder climates, associated with north polar vortex contraction or weaker meridional circulation (22), occurred at about 610 to 960, 1500 to 2700, 6300 to 7900, and 9300 to 10,600 years B.P.

Cold events identified in our glaciochemical series correspond in timing to records of worldwide Holocene glacier advances (4) and to cold events in paleoclimate records from Europe, North America, and the Southern Hemisphere (5), as determined by combining glacier advance, oxygen isotope ($\delta^{18}\text{O}$), pollen count, tree ring width, and ice core data (Fig. 2). Cold

S. R. O'Brien, M. S. Twickler, S. I. Whitlow, Glacier Research Group, Institute for the Study of Earth, Oceans, and Space, University of New Hampshire, Durham, NH 03824, USA.

P. A. Mayewski, Glacier Research Group, Institute for the Study of Earth, Oceans, and Space, and Department of Earth Sciences, University of New Hampshire, Durham, NH 03824, USA.

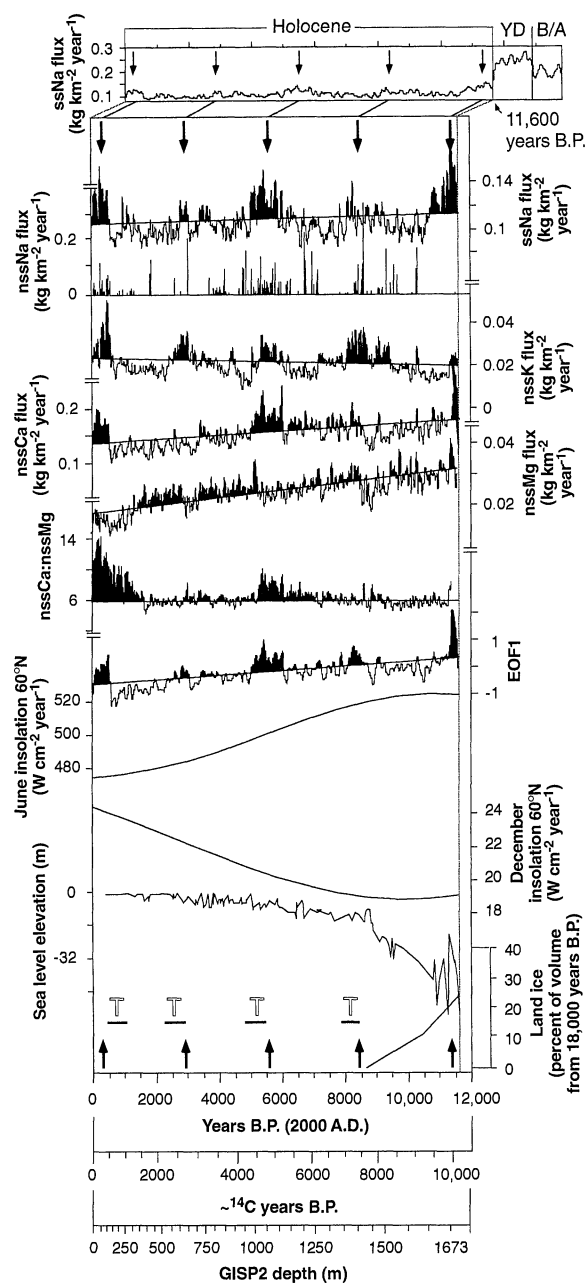
L. D. Meeker, Glacier Research Group, Institute for the Study of Earth, Oceans, and Space, and Department of Mathematics, University of New Hampshire, Durham, NH 03824, USA.

D. A. Meese, Cold Regions Research and Engineering Laboratory, Hanover, NH 03755, USA.

*Present address: Paragon Environmental Services, Inc., 153 Washington, East Walpole, MA 02032, USA.

†To whom correspondence should be addressed.

Fig. 1. Profiles of the GISP2 estimated ss and nss species for the Holocene and potential climate-forcing factors. All profiles are smoothed with a robust spline (equivalent to a 100-year smooth) to be consistent with previously published GISP2 data (3). The ssNa profile represents the behavior of all ss species and is illustrated through the YD and part of the Bolling-Allerod (B/A) events to reference the relatively low Holocene glaciochemical concentrations. The nssCa:nssMg ratio and the Holocene EOF1 (defined in text) are also included. Values above the respective standard linear regressions of each species are shaded, and increases in concentration are marked by arrows. Values above the nssCa:nssMg ratio base line are shaded. Potential climate-forcing factors include insolation (34), and sea level elevation and land ice percentage (14). Episodes of triple oscillations [T (24)] are also indicated. These are defined as $\delta^{14}\text{C}$ intervals which have Maunder- and Spörer-type patterns occurring in sets of three. The most recent triple event (T) corresponds to the Maunder, Spörer, and Wolf solar activity minima. Radiocarbon ($\delta^{14}\text{C}$) dating was determined as described (23).



periods identified in the GISP2 record also correspond in timing to periods of low solar output, as identified in residual tree ring radiocarbon ($\delta^{14}\text{C}$) age measurements (23). Sections of the $\delta^{14}\text{C}$ record containing at least two Maunder- and Spörer-type digressions [referred to as triple oscillations or T events (24)] approximate the timing of century-scale GISP2 glaciochemical increases (Fig. 1). Although a $\delta^{14}\text{C}$ -climate link is controversial, a Holocene climate quasi-cycle of ~2500 years (close to our quasi-2600-year pattern), in phase with $\delta^{14}\text{C}$ variations, has been identified by a number of researchers examining glacial moraines, $\delta^{18}\text{O}$ records from ice cores, and temperature-sensitive tree ring widths (25).

Terrestrial source species provide addi-

tional evidence of changes in atmospheric circulation. Concentrations of nssK and to a lesser degree of nssCa track ssNa events, which suggests that changes in atmospheric circulation affected marine and terrestrial surfaces synchronously. However, air masses reaching Summit ~0 to 1700 years B.P. and ~5200 to 6000 years B.P. passed over terrestrial regions that supplied more Ca relative to Mg (Fig. 1). These changes could represent progressively changing environments or gradual shifts in circulation paths. Although data on the soluble components of Ca and Mg derived from dust sources is limited, the nssCa:nssMg ratios at Summit agree with Ca:Mg ratios obtained from western Tibetan ice cores (26) and from inland U.S. sites (27). The greatest nssCa:nssMg ratio change

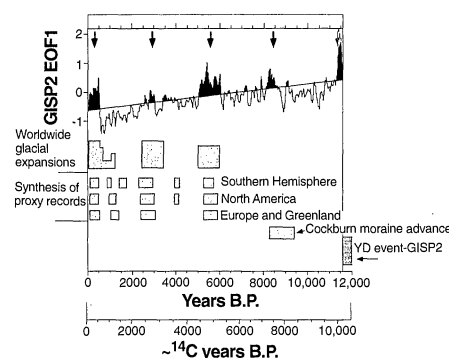


Fig. 2. Paleoclimate cold events: GISP2 Holocene EOF1; worldwide glacial expansions and their relative magnitude (4); synthesis of various climate proxy records from Europe, Greenland, North America, and the Southern Hemisphere showing cold periods (5); the Cockburn Stade (31); and the YD event (10).

was ~300 years ago, perhaps reflecting increases in exposed terrain caused by changes in agricultural practices.

Comparison of the GISP2 glaciochemical series with other Summit, Greenland, ice cores reveals interesting similarities and differences. The GISP2 chemical record, $\delta^{18}\text{O}$ record (28), and accumulation record (29) and the CH_4 record from the Greenland Ice Core Project [GRIP; 28 km east of GISP2 (30)] all indicate a notable period of environmental change that occurred at ~8400 years B.P. A glacial advance in North America, the Cockburn Stade (31), also began at ~8400 years B.P. However, at 5600 years B.P., even though a distinct change is evident in the GISP2 accumulation and glaciochemical records and in the GRIP CH_4 records, no change appears in the GISP2 $\delta^{18}\text{O}$ record (32). Thus, although environmental and climatic changes affected source regions in the mid to high latitudes (GISP2 terrestrial and marine source regions) and in the mid to low latitudes [CH_4 source regions (30)], no substantial change in temperature occurred at Summit ($\delta^{18}\text{O}$ source region). After 5600 years B.P., there are few synchronous anomalies among GISP2 marine-terrestrial species, accumulation rate, and $\delta^{18}\text{O}$ records and GRIP CH_4 records. For example, the accumulation rate does not vary significantly over the LIA (29) even though GISP2 glaciochemical and $\delta^{18}\text{O}$ series show a distinct LIA (32, 33).

We conclude that as the Holocene progressed, environmental change increasingly occurred on a regional basis. This complexity in Holocene climate makes distinguishing natural from anthropogenically altered climate a formidable task.

REFERENCES AND NOTES

1. K. C. Taylor *et al.*, *Nature* **361**, 432 (1992).
2. R. B. Alley *et al.*, *ibid.* **362**, 527 (1993).
3. P. A. Mayewski *et al.*, *Science* **263**, 1747 (1994).

4. G. H. Denton and W. Karlén, *Quat. Res.* **3**, 155 (1973).
5. L. D. D. Harvey, *Prog. Phys. Geogr.* **4**, 487 (1980).
6. J. M. Grove, *The Little Ice Age* (Methuen, London, 1988).
7. Error estimates in the dating of the GISP2 ice core are 2% for 0 to 11,640 years B.P. (2). For a more detailed description of dating methods used on the GISP2 ice core, see D. A. Meese *et al.*, "Preliminary depth-age scale of the GISP2 ice core," *Spec. CRREL Rep. 94-1* (Cold Regions Research and Engineering Laboratory, Hanover, NH, 1994). The time period 11,600 years B.P. corresponds to a core depth of ~1670 m.
8. Sampling and analysis of the core for glaciochemical species required specially adapted techniques to minimize contamination [P. A. Mayewski, M. J. Spencer, M. S. Twickler, S. Whitlow, *Ann. Glaciol.* **14**, 186 (1990); C. F. Buck *et al.*, *J. Chromatogr.* **594**, 225 (1992)].
9. In this model, sea salt components are estimated by an iterative process in which each sample is tested to determine which species is the most conservative (limiting). The limiting ion is then used to derive estimated sea salt concentrations, per sample, for the other species (3). This model assumes that no chemical fractionation occurred during sea salt aerosol formation and transport. Thus, if anything, it underestimates sea salt contributions to Summit snow and overestimates non-sea salt contributions. It is generally accepted that a limited fractionation, if any, of sea salt aerosols (excluding chloride) occurs [for example, R. A. Duce and E. J. Hoffman, *Annu. Rev. Earth Planet. Sci.* **4**, 187 (1976); E. J. Hoffman, G. L. Hoffman, I. S. Fletcher, R. A. Duce, *Atmos. Environ.* **11**, 373 (1977); E. J. Hoffman, G. L. Hoffman, R. A. Duce, *J. Geophys. Res.* **85**, 5499 (1980); D. L. Savoie and J. M. Prospero, *ibid.*, p. 385]. Estimated values of marine source species confirm that most of the Na (>99%) measured in the Holocene portion of the GISP2 core is derived from sea salt, whereas an estimated 73, 35, 19, 3, and 3% of Cl, Mg, K, Ca, and SO_4 , respectively, are derived from sea salt. Sodium was used as the sea salt indicator for 4865 of the 5114 Holocene samples. Chlorine was used as the sea salt indicator for 233 of the samples, Mg for 10 samples, and K for 6 samples.
10. P. A. Mayewski *et al.*, *Science* **261**, 195 (1993).
11. J. P. Peixoto and A. H. Oort, *The Physics of Climate* (American Institute of Physics, New York, 1992).
12. L. D. Meeker, P. A. Mayewski, M. S. Twickler, S. I. Whitlow, in preparation.
13. M. Ters, in *Climate History, Periodicity, and Predictability*, M. R. Rampino, J. E. Sanders, W. S. Newman, L. K. Königsson, Eds. (Van Nostrand Reinhold, New York, 1987), pp. 205–237.
14. At the onset of the Holocene, sea level was about 40 m lower than it is today (13). Sea level is reported to have reached its modern position ~7000 to 8000 years B.P. along the U.S. [D. J. Cloquhoun and M. J. Brooks, in (13), pp. 143–156] and French Atlantic coasts (13). Little land ice was left for melting after ~7500 years B.P. [for example, G. H. Denton and T. J. Hughes, *The Last Great Ice Sheets* (Wiley, New York, 1981)].
15. N. Roberts and R. H. Wright, in *Global Climates Since the Last Glacial Maximum*, H. E. Wright *et al.*, Eds. (Univ. of Minnesota Press, Minneapolis, MN, 1993), pp. 194–220.
16. Results from the "Climates of the Holocene—Mapping Based on Pollen Data" (COHMAP) experiments.
17. J. E. Kutzbach and T. Webb III, in (15), pp. 5–11.
18. C. D. Charles, D. Rind, J. Jouzel, R. D. Koster, R. G. Fairbanks, *Science* **263**, 508 (1994).
19. H. H. Lamb, *Climate History and the Future* (Princeton Univ. Press, Princeton, NJ, 1977), vol. 2. The LIA is a term used widely to describe the cool period between the Middle Ages and the first half of the 20th century.
20. D. J. Erickson, J. T. Merrill, R. A. Duce, *J. Geophys. Res.* **91**, 1067 (1986); S. Whitlow, P. M. Mayewski, J. E. Dibb, *Atmos. Environ. A* **26**, 2045 (1992); D. A. Mosher, P. Winkler, J. Jaffrezo, *ibid.* **27**, 2761 (1993).
21. R. E. Newell and Y. Zhu, *Geophys. Res. Lett.* **21**, 113 (1994).
22. J. F. O'Connor, *Mon. Weather Rev.* **89**, 211 (1961).
23. M. Stuiver and P. J. Reimer, *Radiocarbon* **35**, 215 (1993).
24. M. Stuiver and T. Braziunas, *Nature* **338**, 405 (1989).
25. J. R. Bray, *ibid.* **228**, 353 (1970); (3); D. A. Fisher, *Clim. Change* **4**, 419 (1982); W. Dansgaard, in *Climate Processes and Climate Sensitivity*, J. E. Harness and T. Takahashi, Eds. (Geophysical Monograph, Washington, DC, 1984), vol. 29, pp. 288–298; V. C. LaMarche Jr., *Science* **183**, 1043 (1974).
26. C. P. Wake and P. A. Mayewski, *Tellus B* **46**, 220 (1994).
27. R. A. Berger and W. M. Berger, *The Global Water Cycle—Geochemistry and Environment* (Prentice Hall, Englewood Cliffs, NJ, 1987).
28. P. M. Grootes, M. Stuiver, J. W. White, S. Johnsen, J. Jouzel, *Nature* **366**, 552 (1993).
29. D. A. Meese *et al.*, *Science* **266**, 1680 (1994).
30. T. Blunier, J. Chappellaz, J. Schwander, B. Stauffer, D. Raynaud, *Nature* **374**, 46 (1995).
31. J. T. Andrews and J. D. Ives, in *Climate Changes During the Last 10,000 Years*, Y. Vasari, H. Hyvärinen, S. Hicks, Eds. (Univ. of Oulu, Oulu, Finland, 1972).
32. M. Stuiver, P. M. Grootes, T. F. Braziunas, *Quat. Res.*, in press.
33. P. A. Mayewski *et al.*, *J. Geophys. Res.* **98**, 12839 (1990).
34. A. L. Berger, *Quat. Res.* **9**, 139 (1978).
35. This work is a contribution to the Greenland Ice Sheet Project 2 (GISP2) and was supported by the NSF Office of Polar Programs. We thank our GISP2 and GRIP colleagues, E. Cook, and anonymous reviewers for their useful comments. We also thank the Polar Ice Coring Office (University of Alaska), the GISP2 Science Management Office (University of New Hampshire), and the 109th Air National Guard for their assistance.

13 June 1995; accepted 2 November 1995

Al Coordination Changes in High-Pressure Aluminosilicate Liquids

J. L. Yarger,* K. H. Smith, R. A. Nieman, J. Diefenbacher, G. H. Wolf, B. T. Poe, P. F. McMillan*

Understanding the effect of pressure on aluminosilicate glass and liquid structure is critical to understanding magma flow at depth. Aluminum coordination has been predicted by mineral phase analysis and molecular dynamic calculations to change with increasing pressure. Nuclear magnetic resonance studies of glasses quenched from high pressure provide clear evidence for an increase in the average coordination of Al with pressure.

Many igneous processes are influenced by the properties of molten aluminosilicates at depth (1). The variation in melt density with depth compared with that of the surrounding mantle will ultimately determine the buoyancy forces on the melts. Furthermore, the change in viscosity of the melt with pressure will determine the time scale for melt implantation, mineral crystallization and fractionation, and thermal transport. This has spurred a great deal of interest in understanding the thermodynamic and transport properties of aluminosilicate melts as a function of pressure and temperature.

Consisting of a fully polymerized tetrahedral network, SiO_2 has a high viscosity. Addition of a network modifier, such as Na_2O , breaks the Si–O–Si linkages to form $\text{Si–O}^- \cdots \text{Na}^+$ [nonbridging oxygens (NBOs)] and lowers the viscosity. In contrast, the addition of Al_2O_3 to alkali-silicate melts ($\text{Na}_2\text{O}:\text{Al}_2\text{O}_3 \geq 1$) removes the NBOs and reconstructs the tetrahedral network, increasing the viscosity. Aluminosilicate melts with a high silica content form three-dimensional tetrahedral networks

with extremely high viscosities. However, the viscosity of some highly silicic melts decreases with increasing pressure, so that their mobility at depth can be several orders of magnitude greater. A similar decrease in viscosity occurs in both natural and synthetic aluminosilicate melts, bracketing the entire composition range from andesitic to basaltic magmas (2). This anomalous behavior was first attributed to a pressure-induced increase in the Al coordination and a resultant weakening of the Al–O bond strength, analogous to that occurring in crystalline aluminosilicate minerals at high pressures (3). Subsequent spectroscopic experiments on glasses quenched from high-pressure melts showed no evidence of coordination change. Hence, the observed viscosity decrease was rationalized as bond weakening due to bond angle changes in the aluminosilicate tetrahedral network (4). An early report suggested evidence for six-coordinate Al in ambient albite ($\text{NaAlSi}_3\text{O}_8$) glasses quenched from melts formed at 6 and 8 GPa (5). This was later shown to be due to a trace of high-pressure crystalline material quenched into the glass samples. No definitive evidence has been found in subsequent work for high-coordinate Al sites in (high-silica) aluminosilicate glasses quenched from pressures up to 10 GPa (6).

Nuclear magnetic resonance (NMR) studies have revealed the presence of substantial amounts of high-coordinate Si (Si^{IV}

J. L. Yarger, K. H. Smith, R. A. Nieman, Department of Chemistry and Biochemistry, Arizona State University, Tempe, AZ 85287, USA.

J. Diefenbacher, G. H. Wolf, P. F. McMillan, Material Research Group in High-Pressure Synthesis, Arizona State University, Tempe AZ 85287, USA.

B. T. Poe, Bayerisches Geoinstitut, Universität Bayreuth, Bayreuth, Germany D-95440.

*To whom correspondence should be addressed.